Histochemistry and Cell Biology (2021) 156:301–313
https://doi.org/10.1007/s00418-021-02009-5

ORIGINAL PAPER

CD9-positive cells in the intermediate lobe migrate into the anterior lobe to supply endocrine cells

K. Horiguchi[1] · K. Fujiwara[2] · T. Tsukada[3] · T. Nakakura[4] · S. Yoshida[5] · R. Hasegawa[1] · S. Takigami[1] · S. Ohsako[1]

Accepted: 21 June 2021 / Published online: 29 June 2021

Abstract

The adenohypophysis is composed of the anterior and intermediate lobes (AL and IL), and secretes important hormones for growth, sexual development, metabolism, and reproduction. In the marginal cell layer (MCL) facing Rathke's cleft between the IL and AL, cluster of differentiation (CD) 9-, CD81-, S100β-, and SOX2-quadruple positive (CD9/CD81/S100β/SOX2-positive) cells in the adult IL are settled as tissue-resident stem/progenitor cells supplying hormone-producing cells to the AL. However, it is unclear how CD9/CD81/S100β/SOX2-positive cells in the IL-side MCL migrate into the AL across Rathke's cleft. In the present study, we performed chimeric pituitary tissue culture using S100β/GFP-transgenic rats and Wistar rats, and traced the footprint of S100β/GFP-expressing cells. We detected IL-side S100β/GFP-expressing cells in the AL tissue, demonstrating that these cells migrate from the IL to the AL. However, the cells failed to migrate in the opposite direction. Consistently, scanning electron microscopic analysis revealed well-developed cytoplasmic protrusions in the IL-side MCL, but not in the AL-side MCL, suggesting that IL-side CD9/CD81/S100β/SOX2-positive cells had higher migratory activity. We also searched for a specific marker for IL-side CD9/CD81/S100β/SOX2-positive cells and identified tetraspanin 1 (TSPAN1) from microarray analysis. Downregulation of *Tspan1* by specific siRNA impaired cell migration and significantly reduced expression of snail family transcriptional repressor 2 (*Slug*), a marker of epithelial-mesenchymal transition (EMT). Therefore, CD9/CD81/S100β/SOX2-positive cells in the IL-side MCL can be stem/progenitor cells that provide stem/progenitor cells to the AL-side MCL via SLUG-mediated EMT and cell migration.

Keywords CD9 · CD81 · EMT · Pituitary · Migration · Slug · Stem/progenitor cell

Introduction

The anterior lobe (AL) of the adenohypophysis is an important endocrine organ regulating growth, reproduction, stress response, and metabolism. The adenohypophysis derives from the oral ectoderm, from which the AL and intermediate lobe (IL) are formed, while the posterior lobe (PL) is of neural ectoderm origin. In adults, non-endocrine cells expressing sex-determining region Y-box 2 (SOX2) and S100β proteins are considered tissue-resident stem/progenitor cells, and play a critical role in the maintenance of AL functions by controlling the population of hormone-producing cells. S100β/SOX2-positive cells settle in two different stem/progenitor niches: the marginal cell layer (MCL), facing Rathke's cleft between the IL and AL side, is proposed as a primary niche; and SOX2-positive cell clusters scattered throughout AL parenchyma constitute a secondary niche (Chen et al. 2005; Gremeaux et al. 2012; Vankelecom and Chen 2014; Yoshida et al. 2016a, b). Although S100β/

✉ K. Horiguchi
kota@ks.kyorin-u.ac.jp

1 Laboratory of Anatomy and Cell Biology, Department of Health Sciences, Kyorin University, 5-4-1 Shimorenjaku, Mitaka, Tokyo 181-8612, Japan

2 Department of Biological Science, Faculty of Science, Kanagawa University, 2946 Tsuchiya, Hiratsuka, Kanagawa 259-1293, Japan

3 Department of Biomolecular Science, Faculty of Science, Toho University, 2-2-1 Miyama, Funabashi, Chiba 274-8510, Japan

4 Department of Anatomy, Graduate School of Medicine, Teikyo University, 2-11-1 Kaga, Itabashi, Tokyo 173-8605, Japan

5 Department of Biochemistry, The Jikei University School of Medicine, 3-25-8 Nishi-shinbashi, Minato-ku, Tokyo 105-8461, Japan

SOX2-positive cells in the primary niche are thought to supply stem/progenitor cells to the secondary niche, it is unknown whether there are functional and morphological differences between the AL-side and IL-side MCL.

Recently, we identified tetraspanin family proteins CD9 and CD81 as specific markers for S100β/SOX2-positive cells in the primary and secondary niches, but not for S100β/SOX2-positive pituicytes in the PL (Horiguchi et al. 2018) (Supplementary figure S1). We named these CD9/CD81/S100β/SOX2-positive cells, and established a method to isolate them from AL tissue containing the AL-side MCL and secondary niche, and from IL/PL tissue containing the IL-side MCL using the pluriBead-cascade cell isolation system with anti-CD9 antibody (Horiguchi et al. 2018, 2020a, c, 2021). Furthermore, these cells can differentiate into hormone-producing cells and also endothelial cells after induction (Horiguchi et al. 2018, 2020a, 2020b, 2021). The cells isolated from the IL-side MCL have higher levels of stem/progenitor markers (*Sox2*) and higher pituisphere-forming capacity than those from the AL-side MCL (Horiguchi et al. 2021). Concomitantly, CD9/CD81 double-knockout mice display dysgenesis of the IL-side MCL and atrophy in the AL, with a significant loss of prolactin (PRL) cells (Jin et al. 2018; Horiguchi et al. 2021). These findings suggest that CD9/CD81/S100β/SOX2-positive cells in the IL-side MCL are more immature than those in the AL-side MCL, and could act as core stem/progenitor cells that supply cells to the AL-side MCL. However, the migratory pathway to the AL has not yet been elucidated.

In this work, we aimed to elucidate the migratory route of CD9/CD81/S100β/SOX2-positive cells and to identify morphological differences between cells in the IL and AL sides. We further searched for specific markers for CD9/CD81/S100β/SOX2-positive cells in the IL-side MCL.

Materials and methods

Animals

Male Wistar rats were purchased from Japan SLC, Inc. (Shizuoka, Japan). The day of birth was designated as P0. Wistar-crlj S100β/GFP-TG rats expressing green fluorescent protein (GFP) under the control of the *S100β* promoter were provided by Professor K. Inoue of Saitama University, and were bred in Kanagawa University. Eight- to ten-week-old rats weighing 200–250 g were given ad libitum access to food and water, and housed under a 12-h light/dark cycle. Rats were sacrificed by exsanguination from the right atrium in a deep sleep under three anaesthetics (0.15 mg/kg of medetomidine, Zenyaku Kogyo, Tokyo, Japan, 2.0 mg/kg of midazolam, SANDOZ, Tokyo, Japan, and 2.5 mg/kg of butorphanol, Meiji Seika Pharma, Tokyo, Japan). Then, Hanks' balanced salt solution (Thermo Fisher Scientific, Waltham, MA, USA) and 4% paraformaldehyde in 0.05 M phosphate buffer (PB; pH 7.4) were perfused from the aorta for cell culture and for histological analyses, respectively. The present study was approved by the Committee on Animal Experiments of Kyorin and Kanagawa University, based on the NIH Guidelines for the Care and Use of Laboratory Animals.

Immunohistochemistry and immunocytochemistry

Frozen frontal sections of rat pituitary gland (8 µm thickness) were obtained using a cryostat (Tissue-tek Polar DM; Sakura Finetek, Tokyo, Japan) and immunohistochemistry was performed as described previously (Horiguchi et al. 2014). For immunocytochemistry, cultured cells fixed with 4% paraformaldehyde in 0.025 M PB for 20 min at room temperature (21–23 °C) were first immersed in phosphate-buffered saline (PBS) containing 2% normal goat or donkey serum for 20 min at 30 °C. Primary and secondary antibodies used for immunohistochemistry and immunocytochemistry are listed in Supplementary Table S1. The absence of an observable nonspecific reaction was confirmed using normal mouse, rabbit, donkey, or goat serum (data not shown). Absence of an observable nonspecific immunoreaction against CD9 was also confirmed as described previously (Horiguchi et al. 2021). Briefly, the anti-CD9 antibody was preincubated with a CD9 peptide (ORB217044; Biobyt, Cambridge, U.K.) for 2 days at 4 °C and then centrifuged. The resultant supernatant was used as the pre-adsorbed antibody. Sections were scanned using an epifluorescence microscope (BX61, Olympus, Tokyo, Japan) with the cellSens Dimension system (Olympus).

qPCR

Quantitative polymerase chain reaction (qPCR) was performed as described previously (Horiguchi et al. 2016b). Using TRIzol Reagent (Thermo Fisher Scientific, Carlsbad, CA, USA), total RNA fractions were prepared from CD9-positive and CD9-negative fractions, and were then incubated with RNase-free DNase I (1 U/tube; Promega, Madison, WI, USA) for 10 min at 37 °C. Next, cDNA was synthesized using the PrimeScript RT reagent kit (Takara, Shiga, Japan) with oligo-$(dT)_{20}$ primer (Thermo Fisher Scientific). Briefly, qPCR assays were conducted on a Thermal Cycler Dice Real Time System II (Takara) using gene-specific primers and SYBR Premix Ex Taq II (Takara) containing SYBR Green I. The sequences of the gene-specific primers were as follows: *Slug*, 5′-CATCTGCAGACCCACTCTGA-3′ and 5′-AGCAGCCAGACTCCTCATGT-3′ (product length: 103 bp); *Tspan1*, 5′-ACACCACAATGGCTGAACAA-3′ 5′-CCCTCCATCGTAGAGTTCCA-3′

(product length: 109 bp); *Cd9*, 5′-GGCTATACCCACAAG GACGA-3′5′-GCTATGCCACAGCAGTTCAA-3′ (product length: 140 bp); and β-actin (*Actb*), 5′-TGGCACCACACT TTCTACAATGAGC-3′ and 5′-GGGTCATCTTTTCAC GGTTGG-3′ (product length: 106 bp).

Cultivation of pituitary gland in collagen gel

Pituitary glands of S100β/GFP-TG and Wistar rats at P5 and 9 weeks old (9 W) were sampled. The IL/PL tissue was separated from AL tissue; then, the IL/PL tissue from S100β/GFP-TG rat at P5 or 9 W was placed on the AL tissue of Wistar rats at P5 or 9 W, respectively. Pituitaries were individually placed in collagen type I gel (Nitta Gelatin Inc., Osaka, Japan) on eight-well glass chamber slides (1 cm^2/well; Nalge Nunc International, Rochester, NY, USA) prior to the culture. Pituitaries were then covered with DMEM/F-12 (Life Technologies) with 10% fetal bovine serum (FBS) (Merck Millipore), 0.5 U/mL penicillin, and 0.5 µg/mL streptomycin (Life Technologies) for 2 days at 37 °C in a humidified atmosphere of 5% CO_2 and 95% air. Pituitary glands were carefully dissected out from collagen type I gel and fixed overnight in 4% paraformaldehyde in 0.05 M PB at 4 °C. Tissues were then immersed in PB containing 30% sucrose for 2 days at 4 °C, embedded in Tissue Tek compound (Sakura Finetechnical, Tokyo, Japan) and frozen rapidly. Sectioning and immunohistochemistry were performed as mentioned above. Cultivation was performed three times for each experimental group. After immunohistochemistry, using a 40-fold objective lens (157.5 × 210 µm rectangle), GFP-expressing cells were captured in each section. The number of GFP-expressing cells in sections was counted using the CellSens Dimension system (Olympus). Three individual experiments were carried out for the cell counting.

Scanning electron microscopy

Three pituitary glands at P5 were fixed with 2.5% glutaraldehyde in 0.1 M PB (pH 7.4) for 1 h at 4 °C. Specimens were defatted in 90% ethanol for 2 days after thorough demineralization. Next, specimens were corroded in 10 M sodium hydroxide for 3 days at 60 °C, followed by washing in running water. After critical point drying in CO_2 and coating with platinum in a sputter coater, specimens were observed with an S-4100 electron microscope (Hitachi, Tokyo, Japan).

Isolation of CD9-positive cells

The pituitary glands of the male Wistar rats were dissected, and the AL was manually separated from the pituitary gland by tweezers; AL and IL/PL tissues were enzymatically digested to disperse cells as described previously (Horiguchi et al. 2008). Dispersed cells were counted using a hemocytometer, and CD9-positive cells were separated using a Universal Mouse pluriBeads kit (pluriSelect, San Diego, CA, USA) as described in our previous papers, with a monoclonal anti-rat CD9 antibody (BD Biosciences, San Jose, CA, USA) (Horiguchi et al. 2016b, 2018, 2021). CD9-positive and CD9-negative cells were processed for smear preparation, qPCR, cDNA microarray, or cultivation.

cDNA microarray

The total RNA treated with DNase I was extracted from CD9-positive and CD9-negative cells from IL/PL tissue as described above, and then microarrays were performed by a custom analysis service (Takara) using an Agilent microarray. Microarray data were normalized by median levels.

In situ hybridization

In situ hybridization was performed with digoxigenin (DIG)-labeled complementary RNA (cRNA) probes, as described in our previous report (Horiguchi et al. 2018). A fragment of the *Tspan1* gene was PCR-amplified from the rat pituitary cDNA library using the following primer pair: 5′-ACA CCACAATGGCTGAACAA-3′ and 5′-GGTCCCTAATTA GCCCGAAG-3′ (product length: 548 bp). The amplified cDNA was ligated into the pTA-2 vector (Toyobo) and subcloned into a plasmid vector. Gene-specific antisense and sense DIG-labeled cRNA probes were generated using the Roche DIG RNA Labeling Kit (Roche Diagnostics, Basel, Switzerland). In situ hybridization signals were visualized using the HNPP Fluorescent Detection Kit (Roche Diagnostics). After in situ hybridization, sections were stained using immunohistochemistry, as described above. A control experiment using the sense cRNA probe was performed, and no specific signal was detected. Cells were scanned using a microscope (BX61, Olympus). After immunohistochemistry, five random fields (157.5 × 210 mm rectangle) were captured per section using a 40-fold objective lens. The number of cells positive for TSPAN1, CD9, S100β, and SOX2, and the total number of cells (DAPI) per area were counted with the cellSens Dimension system. Cell counts were performed three times for each experimental group.

Small interfering RNA (siRNA)

CD9-positive cells isolated from the IL of adult Wistar rats were plated in a 96-well chamber with a laminin-coated surface. Cells were then cultured for 72 h in 200 µL Medium 199 with 10% FBS (Merck Millipore) at 37 °C in a humidified atmosphere of 5% CO_2 and 95% air. For transfection of siRNAs, the culture medium was replaced with 200 µL per well of Medium 199 with 10% FBS supplemented with

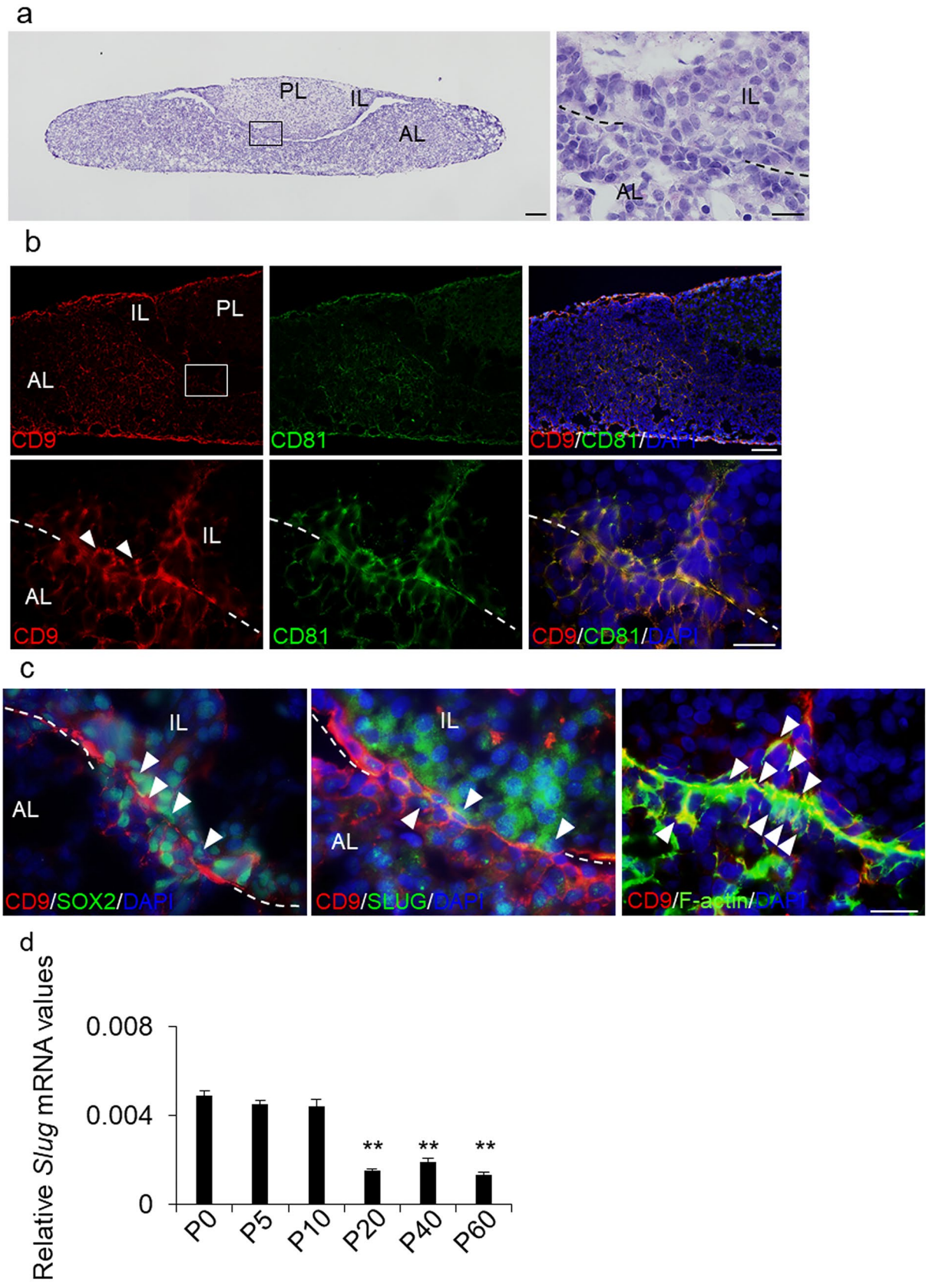
a
PL
IL
AL
IL
AL
b
IL
PL
AL
CD9
CD81
CD9/CD81/DAPI
IL
AL
CD9
CD81
CD9/CD81/DAPI
c
IL
AL
CD9/SOX2/DAPI
IL
AL
CD9/SLUG/DAPI
CD9/F-actin/DAPI
d
Relative Slug mRNA values
0.008
0.004
0
**
**
**
P0
P5
P10
P20
P40
P60

◂**Fig. 1** Identification of CD9- and CD81-positive cells in the pituitary (P5). **a** HE staining of the pituitary gland. Right panel: high magnification of boxed area of left panel. In some areas, cell bridges across Rathke's cleft (RC) between AL and IL were observed. **b** Double immunohistochemistry staining for CD9 (*red*) and CD81 (*green*) with DAPI staining (*blue*). Upper panels: low-magnification images of the pituitary gland. Lower panels: high magnification of boxed area of upper panels. **c** Double immunohistochemistry staining for CD9 (*red*) and SOX2 (*green*, left panel) or SLUG (*green*, middle panel) or F-actin (green, right panel) with DAPI staining (*blue*). **d** mRNA levels of *Slug* in IL-side CD9-positive cells were determined by qPCR (mean ± SEM, $n = 5$), followed by normalization with an internal control (*Actb*). $^{**}P < 0.01$. AL, anterior lobe, IL, intermediate lobe, PL, posterior lobe. Scale bars, 100 µm (**a**, left panel and **b**, upper panel), 50 µm (**a**, right panels, **b**, lower panel, and **c**). Dotted lines show Rathke's cleft. White arrowhead indicates the double positive cells in the cell bridge between the IL and AL

transfection reagent (INTERFERin at 1:100 v/v; PolyPlus Transfection, Illkirch, France) and siRNAs against *Tspan1* mRNA (0.2 µM Rn_RGD:1303308_1; Qiagen, Venlo, Netherlands). The bottom of each well was scratched with a 10 µL pipette tip for the wound healing assay. A non-silencing siRNA without homology to any known mammalian gene was used as a negative control (SI03650325; Qiagen). After 72 h cultivation with siRNA reagents, cells were observed using the cellSens Dimension system (Olympus) and processed for qPCR.

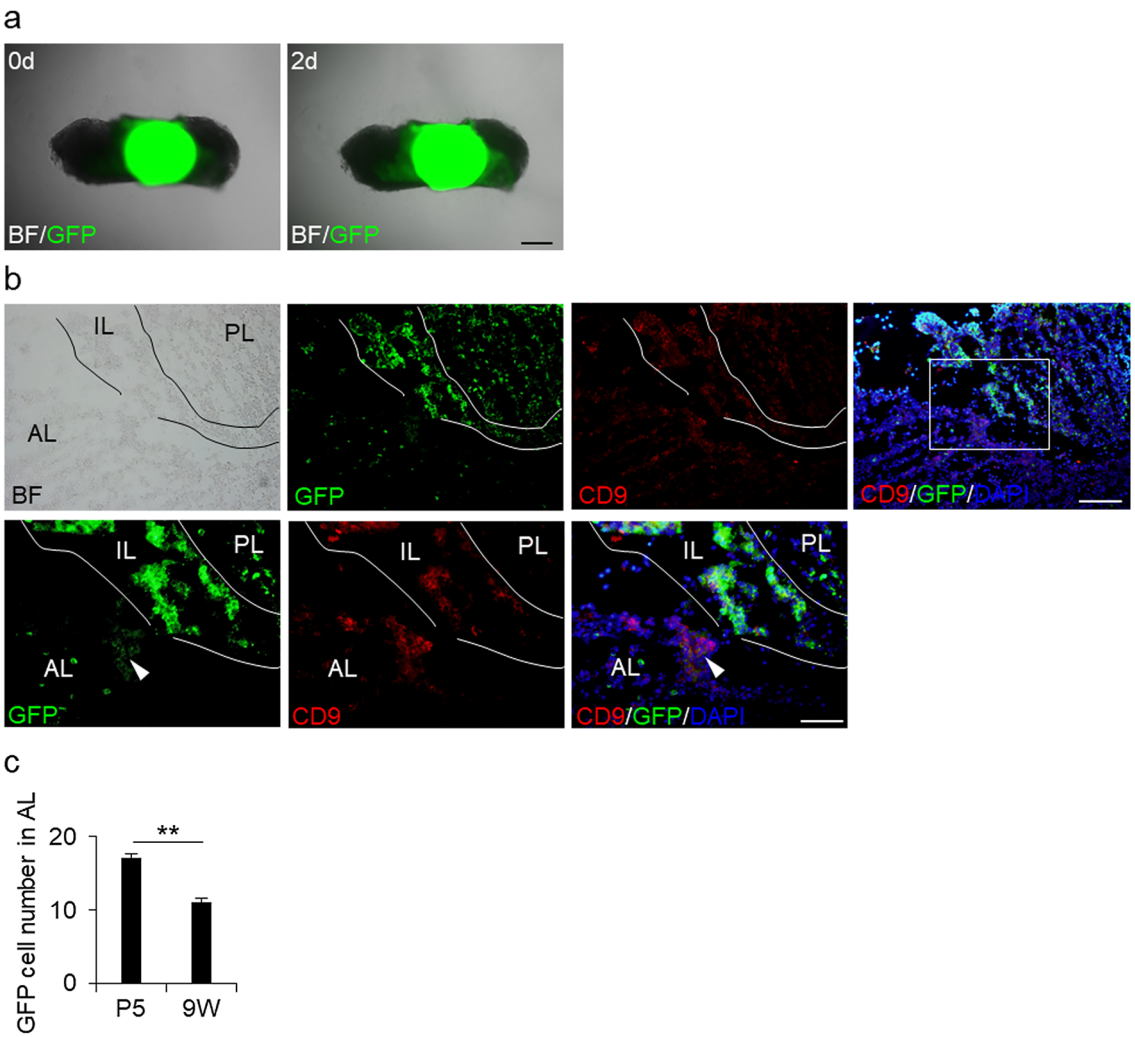

Fig. 2 Migration of GFP-expressing cells of S100β/GFP-TG rats from the IL-side MCL to the AL side of Wistar rats. **a** Merged images of bright field and GFP of chimeric pituitary tissue cultured in collagen type I gel for 0 (left panel, 0d) and 2 (right panel, 2d) days. Fluorescent and non-fluorescent tissues indicate the IL/PL tissue from S100β/GFP-TG rats and the AL tissue from Wistar rats, respectively. **b** Cryosection of chimeric pituitary tissue (2-day cultivation) at P5. Immunohistochemistry for CD9 (*red*), GFP (*green*), and DAPI staining (*blue*). Upper panels: low-magnification images. Lower panels: high magnification of the boxed area in the upper right panel. Arrowheads indicate GFP-expressing cells in AL-side MCL. **c** The number of GFP-expressing cells per sections of S100β/GFP-TG rats from the IL-side MCL to the AL side of Wistar rats at P5 and 9 W, respectively. AL, anterior lobe, IL, intermediate lobe, PL, posterior lobe, BF, bright field. Scale bars, 1 mm (**a**), 200 µm (**b**, upper panel), 50 µm (**c**, lower panel)

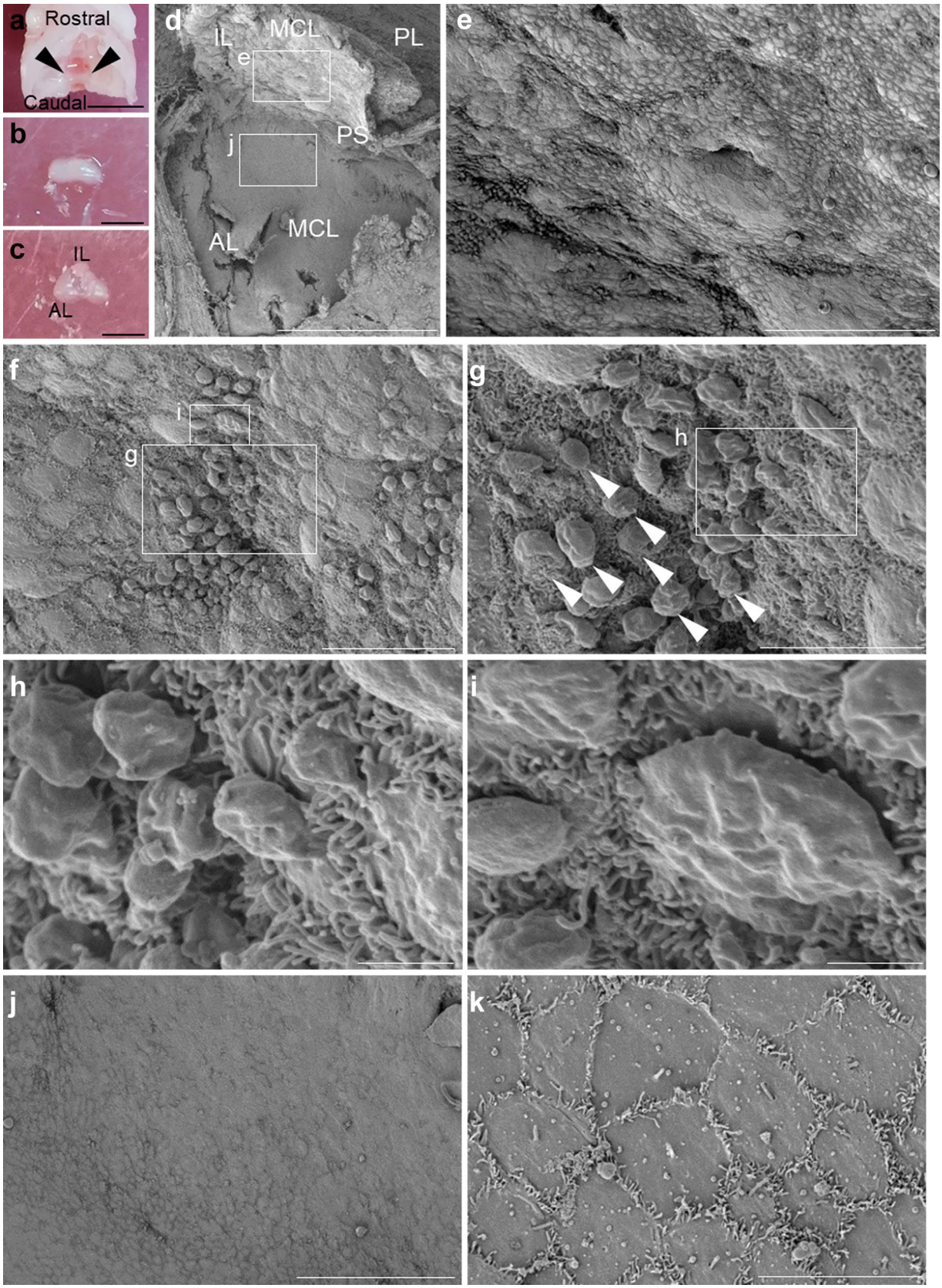
a
Rostral
Caudal
b
c
IL
AL
d
IL
MCL
PL
e
PS
j
AL
MCL
e
f
i
g
g
h
h
i
j
k

◂**Fig. 3** Scanning electron microscopic observation of MCL of pituitary gland (P5). **a** Cerebral base with pituitary gland (arrowheads). **b** Dissected pituitary gland. **c** Flipped IL and PL tissue for preparation of scanning electron microscopy. **d** Low-magnification image of MCL. **e** High magnification of boxed area of (**d**). **f** High magnification of MCL of the IL side. **g** High magnification of boxed area of (**f**). **h** High magnification of boxed area of (**g**). **i** High magnification of boxed area of (**f**). **j** High magnification of boxed area of (**d**). **k** High magnification of AL-side MCL. *MCL* marginal cell layer, *PS* pituitary stalk, *AL* anterior lobe, *IL* intermediate lobe, *PL* posterior lobe. Scale bars, 5 mm (**a**), 2 mm (**b** and **c**), 500 µm (**d**), 100 µm (**e** and **j**), 20 µm (**f**), 10 µm (**g** and **k**), and 2 µm (**h** and **i**)

Statistical analysis

Data are presented as the mean values ± standard error of the mean (SEM) of at least three experiments for each group. Student's *t*-test (after the *F*-test) and the Tukey–Kramer test were used for comparisons between two and more than two groups, respectively. Differences were considered significant at $P < 0.05$.

Results

CD9/CD81/S100β/SOX2-positive cells appear in the pituitary in the postnatal stage

To determine when CD9/CD81/S100β/SOX2-positive cells appear during the pituitary development, we performed immunohistochemistry. CD9- and CD81-positive cells were undetectable during embryonic development (Supplementary figure S2). They started appearing mainly in the IL and in some areas of the AL after birth (Fig. 1). At P5, we observed cell bridges across Rathke's cleft that connected the IL-side and AL-side MCL (Fig. 1a: note that we examined a total of six P5 pituitaries, and cell bridges were observed in all pituitaries). However, the immunopositive cells were densely localized in the bridge area at P5 (Fig. 1b) and co-stained with SOX2, the epithelial-mesenchymal transformation (EMT) marker SLUG (snail family transcriptional repressor 2), and F-actin (Fig. 1c), suggesting that the bridge is a migratory pathway for CD9/CD81/S100β/SOX2-positive cells. qPCR data showed that *Slug* expression was significantly higher in the early postnatal stage (P0–P10) than in the middle–late postnatal stages (P20, P40, and P60) (Fig. 1d).

CD9/CD81/S100β/SOX2-positive cells migrate from IL-side to AL-side MCL

To demonstrate the migration of IL-side CD9/CD81/S100β/SOX2-positive cells into the AL tissue, we swapped IL/PL tissue of Wistar rats with IL/PL tissue of S100β/GFP-TG rats, and then cultured the chimeric tissue for 2 days. For this experiment, we used P5 and 9 W pituitaries (Fig. 2 and Supplemental figure S3a, respectively; strong GFP signals indicate tissue of S100β/GFP-TG rats). After cultivation, the chimeric tissue formed a cell bridge. GFP-positive cells were detected in the AL tissue near the bridge (Fig. 2b: P5, Supplemental figure S3a: 9 W) and expressed CD9 (Fig. 2b). To test whether the GFP-positive cells in the AL can migrate into the IL, we cultured IL/PL tissue of Wistar rats onto the AL tissue of S100β/GFP-TG rats. However, GFP-positive cells were not detected in the IL (Supplemental figure S3b: P5, S3c: 9 W). Next, we counted GFP-positive cells in the anterior lobe of the Wistar rat at P5 and P60. The result showed that migrated cells were higher in the P5 anterior lobe than in the P60 anterior lobe (Fig. 2c). Therefore, CD9/CD81/S100β/SOX2-positive cells are suggested to migrate from the IL to the AL side.

AL- and IL-side MCL cells display morphological differences

As we showed the difference in migratory activity of CD9/CD81/S100β/SOX2-positive cells between the AL and IL side, we performed scanning electron microscopy (SEM) analysis to compare their cell morphology. To this end, we used developing pituitary (P5) and rostrally flipped the IL/PL tissue using forceps prior to SEM preparation (Fig. 3a–c). Micrograph analysis showed that cells in the IL side possessed several cytoplasmic protrusions (Fig. 3e–i, white arrowheads), while cells in the AL side were flat, with no/fewer protrusions (Fig. 3j, k).

TSPAN1 is a cell surface marker of IL-side MCL

Next, we searched for a cell surface marker for IL-side CD9/CD81/S100β/SOX2-positive cells. We first narrowed down candidate membrane proteins from our microarray data that compared gene expression profiles between CD9-positive (CD9+) and CD9-negative (CD9−) fractions from IL/PL tissue, and focused on TSPAN1, as its expression ratio was the highest among tetraspanin family members (Supplementary Table S2). To assess whether TSPAN1 is expressed in IL-side CD9/CD81/S100β/SOX2-positive cells, we employed in situ hybridization and immunohistochemistry. *Tspan1*/TSPAN1-expressing cells were clearly observed in the IL-side MCL but only faintly expressed in the AL side (Fig. 4a, b). Double-staining showed co-localization of *Tspan1* and TSPAN1 (Fig. 4c), confirming the specificity of the TSPAN1 antibody. TSPAN1-positive cells expressed CD9, S100β, and SOX2 (Fig. 4d; the proportions of double-positive cells were 95.6, 90.4, and 87.5%, respectively). The relative expression of *Tspan1* evaluated by qPCR was significantly higher in IL-side than AL-side CD9-positive cells, or than CD9-negative cells in

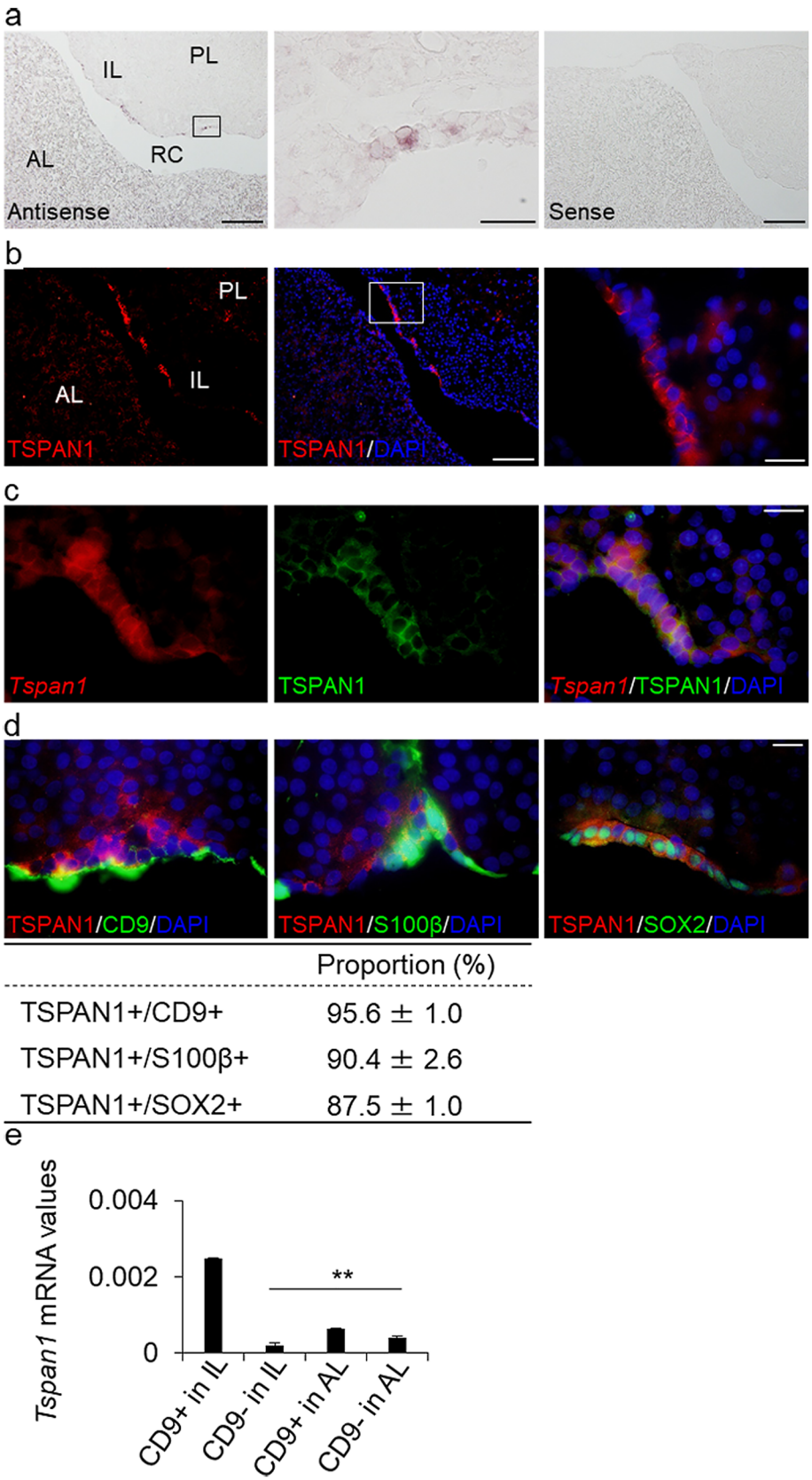

Fig. 4 Identification of TSPAN1 in the pituitary gland. **a** In situ hybridization for *Tspan1* by antisense (left panel) and sense (right panel) probes. Middle panel is high magnification of boxed area of left panel. **b** Immunohistochemistry for TSPAN1 (left panel, *red*) with DAPI staining (middle panel, *blue*) in the pituitary gland. Right panel is high magnification of boxed area of middle panel. **c** In situ hybridization for *Tspan1* (*red*) and immunohistochemistry for TSPAN1 (*green*). **d** Double immunostaining for TSPAN1 (*red*) and either CD9 (*green*), S100β (*green*), or SOX2 (*green*) with DAPI staining (*blue*). Proportions of TSPAN1-positive cells among CD9, S100β, or SOX2-positive cells are shown in the bottom table (mean ± SEM, $n = 5$). **e** Relative mRNA level of *Tspan1* in CD9-positive and CD9-negative cells from IL/PL tissue (*CD9+ in IL* and *CD9− in IL*) and AL (*CD9+ in AL* and *CD9− in AL*). Data were normalized with an internal control (*Actb*) (mean ± SEM, $n = 3$). *AL* anterior lobe, *IL* intermediate lobe, *PL* posterior lobe, *RC* Rathke's cleft. Scale bars, 200 µm (a, left panel and b, middle panel), 100 µm (a, right panel), 20 µm (**a**, middle panel, **b**, right panel, **c**, right panel, and **d** right panel)

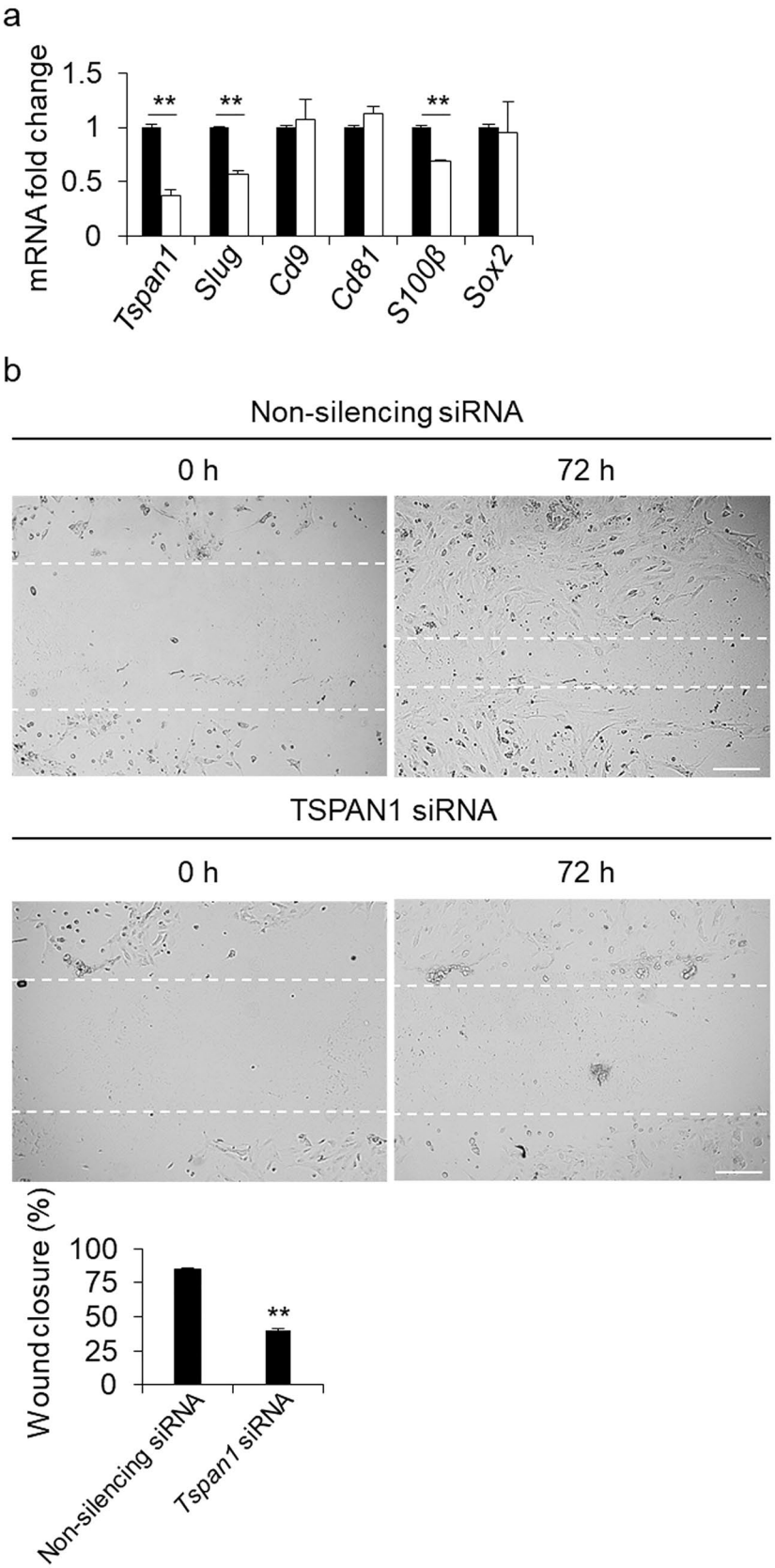

Fig. 5 Wound healing assay using *Tspan1* siRNA-treated cells. **a** Relative mRNA level of *Tspan1* and *Slug* in CD9/CD81/S100β/SOX2-positive cells of the IL after 72 h treatment with non-silencing siRNAs (*white*) and *Tspan1* siRNA (*black*) (mean ± SEM, $n = 3$). **b** Bright image of CD9-positive cells after 0 and 72 h treatment with non-silencing siRNAs and *Tspan1* siRNA. Lower graph shows relative invasion area after 72 h treatment with non-silencing siRNAs and *Tspan1* siRNA by wound healing assay

both the AL and IL (Fig. 4e). These results strongly support the idea that TSPAN1 could be a cell surface marker for IL-side CD9/CD81/S100β/SOX2-positive cells. Supplementary figure S4 shows the distribution of TSPAN1 during pituitary development. TSPAN1 was detected in the adenohypophyseal placode at E12.5. After Rathke's pouch was formed, TSPAN1-positive cells were mainly located in the IL at E15.5 and E20.5. However, TSPAN1-positive cells were observed to a similar extent in the AL-side MCL only during the early postnatal period (P5 and P20).

Tspan1 deficiency decreases the invasive ability of CD9/CD81/S100β/SOX2-positive cells

To examine the function of TSPAN1 in the MCL of the IL-side, the *Tspan1* gene in the IL-side CD9/CD81/S100β/SOX2-positive cells was knocked down using siRNAs. *Tspan1* was confirmed to be downregulated by treatment with *Tspan1* siRNA (Fig. 5a). Downregulation of *Slug* and *S100β* was observed in *Tspan1* siRNA-treated cells (Fig. 5a). *Cd9*, *Cd81*, and *Sox2* mRNA levels remained unchanged (Fig. 5a). Subsequent wound healing assays showed significantly lower invasive ability in *Tspan1* siRNA-treated cells than in control siRNA-treated cells (Fig. 5b).

Discussion

The present study revealed that CD9/CD81/S100β/SOX2-positive cells in the IL-side MCL have migratory capacity, with well-developed cytoplasmic protrusions, and may migrate into the AL-side MCL (Fig. 6). We also identify TSPAN1 as a novel marker for CD9/CD81/S100β/SOX2-positive cells in the adult IL-side MCL, which is implicated in SLUG-mediated cell migration.

A previous study proposed that cells in the primary niche (MCL) migrate into the secondary niches (AL parenchyma) to supply stem/progenitor cells, while the cells in the secondary niches migrate into the glandular area to differentiate into hormone-producing cells by EMT (Vankelecom and Chen 2014). However, until now, the cell migration process of stem/progenitor cells in the MCL had not been demonstrated. Here, we performed chimeric pituitary tissue culture using S100β/GFP-TG rat and Wistar rat pituitaries, and traced the S100β/GFP-expressing cells of the IL-side MCL. Within 2 days of cultivation, we observed formation of a cell bridge across Rathke's cleft between the IL and AL, and the presence of IL-side S100β-GFP-expressing cells in the AL-side MCL. On the other hand, AL-side S100β-GFP-expressing cells failed to migrate into the IL. The present study also revealed that CD9/CD81/S100β/SOX2-positive cells in the IL-side MCL highly expressed the EMT marker SLUG and F-actin, especially at the early postnatal stage (P0–10), and possessed developed cytoplasmic protrusions, unlike the smooth cell surface of the AL-side cells. Thus, our experiments first identified the difference in morphology and function between the IL-side and AL-side MCL, and experimentally verified the migratory capacity of CD9/CD81/S100β/SOX2-positive cells in the IL-side MCL. As our recent report showed higher expression levels of stem cell markers (*Sox2* and *S100b*) and pituisphere-forming capacity in CD9/CD81/S100β/SOX2-positive cells in the IL-side MCL than in the AL-side MCL (Horiguchi et al. 2021), CD9/CD81/S100β/SOX2-positive cells in the IL-side MCL may be more immature and have higher migratory activity than their AL-side counterparts. Thus, CD9/CD81/S100β/SOX2-positive cells appear to migrate in stepwise fashion

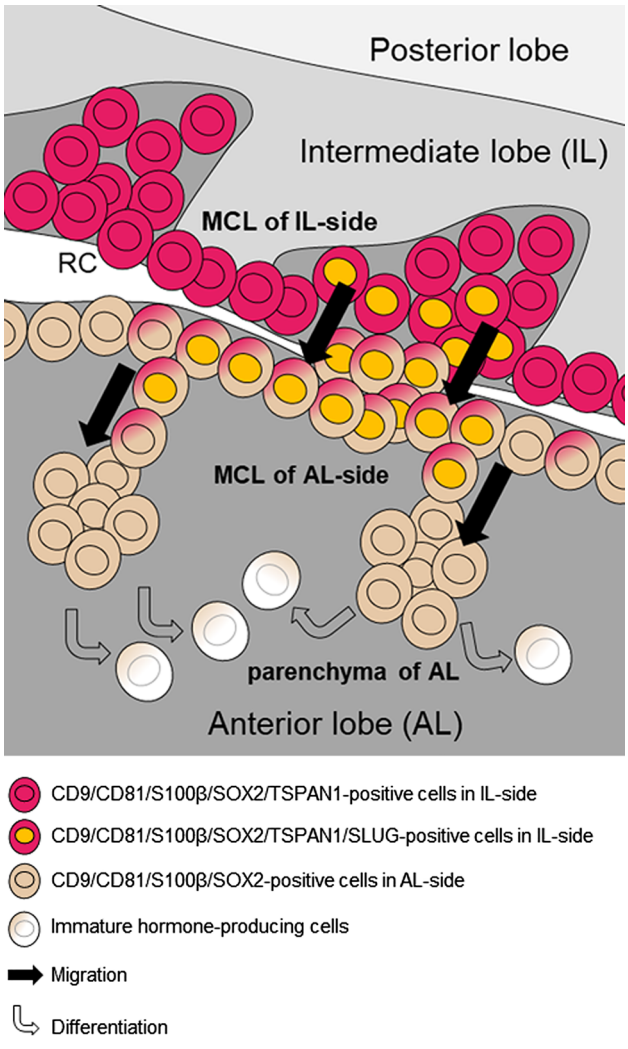

Fig. 6 Schematic of the pituitary stem/progenitor cell niches and the migratory process proposed in the present study. CD9/CD81/S100β/SOX2-positive cells in the IL-side MCL are core stem/progenitor cells in the MCL (primary niche). They migrate into the AL-side MCL (secondary niche) and then into the parenchyma of the AL (third niche). Stem/progenitor cells in the third niche migrate into the glandular area for differentiation into hormone-producing cells

(IL-side MCL, AL-side MCL, and then AL parenchyma) by changing their cell properties towards more committed progenitor cells (Fig. 6).

Jin et al. (2018) showed that CD9/CD81 DKO adult mice exhibit AL atrophy and lack of acidophilic cell number development in the AL. Our further histological investigation using DKO mice revealed that the IL-side MCL was replaced with connective tissue, and that the proportion of PRL cells in the AL was decreased (Horiguchi et al. 2021). However, the AL of the DKO mice possessed all types of hormone-producing cells. These results indicate that CD9/CD81/S100β/SOX2-positive cells could be one of the stem/progenitor cell sources in the AL. Indeed, during early embryonic development of the pituitary gland, CD9-negative SOX2-positive cells first appear in the pituitary primordium and settle in the primary niche, while CD9/CD81/S100β/SOX2-positive cells come into the MCL after birth and increase in cell number during the early postnatal pituitary growth wave (Chen et al. 2013; Horiguchi et al. 2016a, 2021; Yoshida et al. 2011). Therefore, there are at least two different SOX2 stem/progenitor cells in the MCL that are defined by the presence/absence of CD9 expression. Hormone-producing cells in CD9/CD81 DKO mice could be derived from CD9-negative SOX2-positive cells. On the other hand, migration of CD9/CD81/S100β/SOX2-positive cells from the IL side to the AL side was seen even when we used adult pituitary, suggesting they might supply stem/progenitor cells to the secondary niches continuously in the adult stage as tissue-resident stem/progenitor cells.

The present study identified TSPAN1 as a marker of CD9/CD81/S100β/SOX2-positive cells in the IL-side MCL. TSPAN1 is a member of the TSPAN family proteins, which aggregate with various transmembrane receptors, such as integrins, to form TSPAN-enriched microdomains. They are essential in determining cell motility (Detchokul et al. 2014). Our previous study confirmed that integrins, which are cell adhesion receptors constituted by transmembrane α and β heterodimers, are expressed in S100β/SOX2-positive cells (Horiguchi et al. 2010, 2011). Integrins recognize the extracellular matrix (ECM) to activate further intracellular signalling for EMT (Gahmberg et al. 2009), and TSPAN1-integrin microdomains are known to promote EMT (Wang et al. 2018; Liu et al. 2019). Therefore, the migration of CD9/CD81/S100β/SOX2-positive cells shown in the present study may be attributable to the EMT. In addition, downregulation of TSPAN1 in CD9/CD81/S100β/SOX2-positive cells decreased cell motility, accompanied by concomitant downregulation of *Slug* expression. SLUG induces cell migration and division during development, and is also a key modulator of the downregulation of cell adhesion molecule E-cadherin and upregulation of matrix-metalloproteases (MMPs) and CXCL12 (Joseph et al. 2009; Jorda et al. 2005; Shields et al. 2012; Nieto 2002). In our previous study, we confirmed this cascade in S100β-positive cells, showing that SLUG enhances the migration and proliferation activity of S100β-positive cells through upregulation of MMP9, MMP14, and CXCL12, and downregulation of E-cadherin (Horiguchi et al. 2016a). In the present study, downregulation of *S100β* was observed in *Tspan1* siRNA-treated cells. It is possible that TSPAN1 is responsible for SLUG-mediated cell migration and differentiation into hormone-producing cells in CD9/CD81/S100β/SOX2-positive cells.

In summary, the present study hypothesized that CD9/CD81/S100β/SOX2-positive cells in the IL-side MCL are stem/progenitor cells that supply stem/progenitor cells to the AL-side MCL via SLUG-mediated migration through EMT (Fig. 6). As IL-side CD9/CD81/S100β/SOX2-positive cells isolated from adult pituitary still sustained their stemness and differentiation capacity, these cells may constitute an adult tissue-resident stem cell niche in the pituitary which is essential in sustaining endocrine functions in the adult AL by controlling turnover of hormone-producing cells.

Supplementary Information The online version contains supplementary material available at https://doi.org/10.1007/s00418-021-02009-5.

Acknowledgements We are grateful to Dr. Y. Kato and T. Kato (Institute for Reproduction and Endocrinology, Meiji University) for helpful discussions. We would like to thank Editage (www.editage.jp) for English language editing.

Funding This work was supported by JSPS KAKENHI Grants (nos. 19K07255 to K.H.).

Conflicts of interest None.

Availability of data and material Not applicable.

Code availability Not applicable.

Compliance with ethical standards

Disclosure statement The authors have nothing to declare.

Ethical approval The current study was approved by the Committee on Animal Experiments of the Kyorin University based on the NIH Guidelines for the Care and Use of Laboratory Animals. This article does not contain any studies with human participants performed by any of the authors.

References

Chen J, Hersmus N, Van Duppen V, Caesens P, Denef C, Vankelecom H (2005) The adult pituitary contains a cell population displaying stem/progenitor cell and early embryonic characteristics. Endocrinol 146(9):3985–3998. https://doi.org/10.1210/en.2005-0185

Chen M, Kato T, Higuchi M, Yoshida S, Yako H, Kanno N, Kato Y (2013) Coxsackievirus and adenovirus receptor-positive cells compose the putative stem/progenitor cell niches in the marginal cell layer and parenchyma of the rat anterior pituitary. Cell Tissue Res 354(3):823–836. https://doi.org/10.1007/s00441-013-1713-8

Detchokul S, Williams ED, Parker MW, Frauman AG (2014) Tetraspanins as regulators of the tumour microenvironment: implications for metastasis and therapeutic strategies. Br J Pharmacol 171(24):5462–5490. https://doi.org/10.1111/bph.12260

Gahmberg CG, Fagerholm SC, Nurmi SM, Chavakis T, Marchesan S, Gronholm M (2009) Regulation of integrin activity and signalling. Biochim Biophys Acta 1790(6):431–444. https://doi.org/10.1016/j.bbagen.2009.03.007

Gremeaux L, Fu Q, Chen J, Vankelecom H (2012) Activated phenotype of the pituitary stem/progenitor cell compartment during the early-postnatal maturation phase of the gland. Stem Cells Dev 21(5):801–813. https://doi.org/10.1089/scd.2011.0496

Horiguchi K, Fujiwara K, Kouki T, Kikuchi M, Yashiro T (2008) Immunohistochemistry of connexin 43 throughout anterior pituitary gland in a transgenic rat with green fluorescent protein-expressing folliculo-stellate cells. Anat Sci Int 83(4):256–260. https://doi.org/10.1111/j.1447-073X.2008.00239.x

Horiguchi K, Kikuchi M, Kusumoto K, Fujiwara K, Kouki T, Kawanishi K, Yashiro T (2010) Living-cell imaging of transgenic rat anterior pituitary cells in primary culture reveals novel characteristics of folliculo-stellate cells. J Endocrinol 204(2):115–123. https://doi.org/10.1677/joe-09-0333

Horiguchi K, Kouki T, Fujiwara K, Kikuchi M, Yashiro T (2011) The extracellular matrix component laminin promotes gap junction formation in the rat anterior pituitary gland. J Endocrinol 208(3):225–232. https://doi.org/10.1677/joe-10-0297

Horiguchi K, Fujiwara K, Yoshida S, Higuchi M, Tsukada T, Kanno N, Yashiro T, Tateno K, Osako S, Kato T, Kato Y (2014) Isolation of dendritic-cell-like S100beta-positive cells in rat anterior pituitary gland. Cell Tissue Res 357(1):301–308. https://doi.org/10.1007/s00441-014-1817-9

Horiguchi K, Fujiwara K, Tsukada T, Yako H, Tateno K, Hasegawa R, Takigami S, Ohsako S, Yashiro T, Kato T, Kato Y (2016a) Expression of Slug in S100beta-protein-positive cells of postnatal developing rat anterior pituitary gland. Cell Tissue Res 363(2):513–524. https://doi.org/10.1007/s00441-015-2256-y

Horiguchi K, Nakakura T, Yoshida S, Tsukada T, Kanno N, Hasegawa R, Takigami S, Ohsako S, Kato T, Kato Y (2016b) Identification of THY1 as a novel thyrotrope marker and THY1 antibody-mediated thyrotrope isolation in the rat anterior pituitary gland. Biochem Biophys Res Commun 480(2):273–279. https://doi.org/10.1016/j.bbrc.2016.10.049

Horiguchi K, Fujiwara K, Yoshida S, Nakakura T, Arae K, Tsukada T, Hasegawa R, Takigami S, Ohsako S, Yashiro T, Kato T, Kato Y (2018) Isolation and characterisation of CD9-positive pituitary adult stem/progenitor cells in rats. Sci Rep 8(1):5533. https://doi.org/10.1038/s41598-018-23923-0

Horiguchi K, Fujiwara K, Yoshida S, Tsukada T, Hasegawa R, Takigami S, Ohsako S, Yashiro T, Kato T, Kato Y (2020a) CX3CL1/CX3CR1-signalling in the CD9/S100beta/SOX2-positive adult pituitary stem/progenitor cells modulates differentiation into endothelial cells. Histochem Cell Biol 153(6):385–396. https://doi.org/10.1007/s00418-020-01862-0

Horiguchi K, Yoshida S, Tsukada T, Fujiwara K, Nakakura T, Hasegawa R, Takigami S, Ohsako S (2020b) Cluster of differentiation (CD) 9-positive mouse pituitary cells are adult stem/progenitor cells. Histochem Cell Biol 155(3):391–404. https://doi.org/10.1007/s00418-020-01943-0

Horiguchi K, Yoshida S, Tsukada T, Nakakura T, Fujiwara K, Hasegawa R, Takigami S, Ohsako S (2020c) Expression and functions of cluster of differentiation 9 and 81 in rat mammary epithelial cells. J Reprod Dev 66(6):515–522. https://doi.org/10.1262/jrd.2020-082

Horiguchi K, Fujiwara K, Takeda Y, Nakakura T, Tsukada T, Yoshida S, Hasegawa R, Takigami S, Ohsako S (2021) CD9-positive cells in the intermediate lobe of the pituitary gland are important supplier for prolactin-producing cells in the anterior lobe. Cell Tissue Res. https://doi.org/10.1007/s00441-021-03460-5

Jin Y, Takeda Y, Kondo Y, Tripathi LP, Kang S, Takeshita H, Kuhara H, Maeda Y, Higashiguchi M, Miyake K, Morimura O, Koba T, Hayama Y, Koyama S, Nakanishi K, Iwasaki T, Tetsumoto S, Tsujino K, Kuroyama M, Iwahori K, Hirata H, Takimoto T, Suzuki M, Nagatomo I, Sugimoto K, Fujii Y, Kida H, Mizuguchi K, Ito M, Kijima T, Rakugi H, Mekada E, Tachibana I, Kumanogoh A (2018) Double deletion of tetraspanins CD9 and CD81 in mice leads to a syndrome resembling accelerated aging. Sci Rep 8(1):5145. https://doi.org/10.1038/s41598-018-23338-x

Jorda M, Olmeda D, Vinyals A, Valero E, Cubillo E, Llorens A, Cano A, Fabra A (2005) Upregulation of MMP-9 in MDCK epithelial cell line in response to expression of the Snail transcription factor. J Cell Sci 118(Pt 15):3371–3385. https://doi.org/10.1242/jcs.02465

Joseph MJ, Dangi-Garimella S, Shields MA, Diamond ME, Sun L, Koblinski JE, Munshi HG (2009) Slug is a downstream mediator of transforming growth factor-beta1-induced matrix metalloproteinase-9 expression and invasion of oral cancer cells. J Cell Biochem 108(3):726–736. https://doi.org/10.1002/jcb.22309

Liu G, Wang Y, Yang L, Zou B, Gao S, Song Z, Lin Z (2019) Tetraspanin 1 as a mediator of fibrosis inhibits EMT process and Smad2/3 and beta-catenin pathway in human pulmonary fibrosis. J Cell Mol Med 23(5):3583–3596. https://doi.org/10.1111/jcmm.14258

Nieto MA (2002) The snail superfamily of zinc-finger transcription factors. Nat Rev Mol Cell Biol 3(3):155–166. https://doi.org/10.1038/nrm757

Shields MA, Krantz SB, Bentrem DJ, Dangi-Garimella S, Munshi HG (2012) Interplay between beta1-integrin and Rho signaling regulates differential scattering and motility of pancreatic cancer cells by snail and Slug proteins. J Biol Chem 287(9):6218–6229. https://doi.org/10.1074/jbc.M111.308940

Vankelecom H, Chen J (2014) Pituitary stem cells: where do we stand? Mol Cell Endocrinol 385(1–2):2–17. https://doi.org/10.1016/j.mce.2013.08.018

Wang Y, Liang Y, Yang G, Lan Y, Han J, Wang J, Yin D, Song R, Zheng T, Zhang S, Pan S, Liu X, Zhu M, Liu Y, Cui Y, Meng F, Zhang B, Liang S, Guo H, Liu Y, Hassan MK, Liu L (2018) Tetraspanin 1 promotes epithelial-to-mesenchymal transition and metastasis of cholangiocarcinoma via PI3K/AKT signaling. J Exp Clin Cancer Res 37(1):300. https://doi.org/10.1186/s13046-018-0969-y

Yoshida S, Kato T, Yako H, Susa T, Cai LY, Osuna M, Inoue K, Kato Y (2011) Significant quantitative and qualitative transition in pituitary stem / progenitor cells occurs during the postnatal development of the rat anterior pituitary. J Neuroendocrinol 23(10):933–943. https://doi.org/10.1111/j.1365-2826.2011.02198.x

Yoshida S, Kato T, Kato Y (2016a) Regulatory System for Stem/Progenitor Cell Niches in the Adult Rodent Pituitary. Int J Mol Sci 17(1):75. https://doi.org/10.3390/ijms17010075

Yoshida S, Nishimura N, Ueharu H, Kanno N, Higuchi M, Horiguchi K, Kato T, Kato Y (2016b) Isolation of adult pituitary stem/progenitor cell clusters located in the parenchyma of the rat anterior lobe. Stem Cell Res 17(2):318–329. https://doi.org/10.1016/j.scr.2016.08.016